Journal of Solid State Chemistry **162,** 84–89 (2001)
doi:10.1006/jssc.2001.9351, available online at http://www.idealibrary.com on IDEAL®

Magnetic Properties of $La_{1-x}Pr_xCrO_3$

K. Yoshii,*,[1] A. Nakamura,† Y. Ishii,‡ and Y. Morii‡

*Synchrotron Radiation Research Center, Japan Atomic Energy Research Institute (JAERI), Mikazuki, Hyogo 679-5148, Japan; and †Department of Materials Science, and ‡Advanced Science Research Center, Japan Atomic Energy Research Institute (JAERI), Tokai, Ibaraki 319-1195, Japan

Received April 30, 2001; in revised form July 30, 2001; accepted August 9, 2001

Magnetic properties have been investigated for the perovskite $La_{1-x}Pr_xCrO_3$ ($0 \le x \le 1$), which is a solid solution series between $LaCrO_3$ ($x = 0$) and $PrCrO_3$ ($x = 1$), based on dc magnetization and neutron diffraction measurements. The crystal structures were assigned to an orthorhombic perovskite type (space group *Pnma*) in the whole composition region. Canted-antiferromagnetic order is commonly observed at the Néel temperatures (T_N) of 288–240 K. In low applied magnetic fields ($\lesssim$5000 Oe), the solid solutions with a wide composition range of $0.2 \le x \le 0.8$ exhibit distinct negative magnetization below the compensation temperatures (T_{comp}) ($\lesssim$230 K). It is characteristic that the absolute values of such magnetization are much larger (by $\sim$250 times in the largest case with the applied field of 100 Oe) than the positive ordered magnetization observed between T_N and T_{comp}. Neutron diffraction data for $La_{0.5}Pr_{0.5}CrO_3$ showed the existence of G_y-type (G_z for *Pbnm*) antiferromagnetic order of Cr^{3+} moments with no crystallographic change below T_N. Considering the fact that the present behavior is similar to that in $GdCrO_3$, this is plausibly ascribed to the antiparallel coupling of the Pr^{3+} moments and the canted Cr^{3+} moments.

Key Words: **perovskite; chromium oxide; negative magnetization (reversal of magnetization).**

1. INTRODUCTION

Perovskite chromium oxides $LnCrO_3$ (*Ln*, lanthanides) have an orthorhombic perovskite structure at room temperature (space group *Pnma*). They exhibit so-called canted-antiferromagnetic order of localized Cr^{3+} moments ($3d^3$) with Néel temperatures (T_N) of 112–282 K (1–8). Magnetic properties of these systems have been investigated in detail in the past several decades. Very recently, we reported distinct negative magnetization (reversal of magnetization) in a field-cooled process for $La_{0.5}Pr_{0.5}CrO_3$ ($T_N \sim 260$ K), which is the solid solution between two such compounds, $LaCrO_3$ ($T_N \sim 288$ K) and $PrCrO_3$ ($T_N \sim 240$ K) (9). The maximum absolute value of the negative magnetization (at 2 K) is $\sim$40 times as large as that of positive magnetization (at $\sim$220 K). This phenomenon was assumed to arise from the same type of magnetic interaction as in an isostructural compound, $GdCrO_3$ (8), i.e., opposite direction of the Pr^{3+} moments ($4f^2$; effective paramagnetic moment $\mu_{eff} = 3.62\ \mu_B$ (10)) to that of the canted Cr^{3+} moment. It has also been reported that $GdCrO_3$ also exhibits negative magnetization at low temperatures, whose maximum absolute value (at $\sim$25 K) is $\sim$30 times as large as that of the positive magnetization (11). The present paper reports magnetic properties of the system $La_{1-x}Pr_xCrO_3$ ($0 \le x \le 1$) including $La_{0.5}Pr_{0.5}CrO_3$, studied by dc magnetization measurements. Neutron diffraction experiments have also been carried out for $La_{0.5}Pr_{0.5}CrO_3$ at low temperatures.

2. EXPERIMENTAL

The samples have been prepared in air by a solid-state reaction as noted previously using La_2O_3 (4 N, Soekawa), Pr_2O_3 (3 N, Soekawa), and Cr_2O_3 (4 N, Soekawa) as the starting materials (9). The x values for $La_{1-x}Pr_xCrO_3$ were 0, 0.1, 0.2, 0.4, 0.5, 0.6, 0.8, 0.9, and 1. Two to three samples were prepared for each composition and were verified to show reproducible structural and magnetic properties. Five samples were prepared for $x = 0.5$ at the final firing temperatures between 1350 and 1500°C, which showed essentially the same magnetic properties. Though the preheating process on the initial mixtures at 1100°C was adopted in Ref. (9), essentially the same structural and magnetic properties were obtained even if this process was ignored. The crystal structure was determined by powder XRD (X-ray diffraction) measurements. dc Magnetization measurements were performed with a SQUID magnetometer (Quantum Design MPMS) between 2 and 400 K. Magnetization–temperature (M–T) curves were measured in both ZFC (zero-field-cooled) and FC (field-cooled) modes. In the former case, measurements were performed upon cooling with the field, except for applied fields (H) of $H \le 1000$ Oe, where distinct negative magnetization is observed; measurements both

[1]To whom correspondence should be addressed. Fax: +81-791-58-2740. E-mail: yoshiike@spring8.or.jp.

0022-4596/01 $35.00

upon cooling and upheating were done. The results in both kinds of measurements have been found to be essentially identical.

Powder neutron diffraction data were measured for $La_{0.5}Pr_{0.5}CrO_3$ with a high-resolution powder diffractometer (HRPD) at the JRR-3M reactor of JAERI with a neutron wavelength $\lambda = 1.8237$ Å using a Ge(331) monochromator. The experiments were carried out at room temperature, 220 K, 170 K, and 4 K with diffraction angles 2θ between $\sim 10^\circ$ and $\sim 160^\circ$ and an angle step of 0.05°. The patterns obtained were fitted in a 2θ range between 10° and 120° by the Rietveld method using the program RIETAN-2000 (12). Other details have been reported elsewhere (9, 11).

3. RESULTS AND DISCUSSION

Figure 1 shows the lattice parameters and the cell volume for all the compounds plotted against the Pr content (x), which were calculated from the Rietveld method noted in Ref. (9). The space group assumed is orthorhombic *Pnma* as for the end compounds. The XRD patterns were verified to consist only of the reaction products and had analogous profiles to that for $x = 0.5$ (9). Reliability factors (R) and the goodness-of-fit (S) indicators were up to $\sim 15\%$ and ~ 1.45, respectively. Other fitting parameters such as atomic positions are comparable to those for $LaCrO_3$ (7). It was confirmed that lattice parameters of the end compounds were close to those reported previously (1–4, 6, 7). The obtained parameters are $a = 5.4803(1)$ Å, $b = 7.7597(1)$ Å, and $c = 5.5165(1)$ Å for $LaCrO_3$ and $a = 5.4805(1)$ Å, $b = 7.7153(1)$ Å, and $c = 5.4500(1)$ Å for $PrCrO_3$. All the parameters change almost continuously against x, indicating the continuous formation of the solid solutions, though only the a length shows a very slight minimum around $x = 0.5$. It is also noticed that the lattice volume changes almost linearly with x due to the lanthanide contraction.

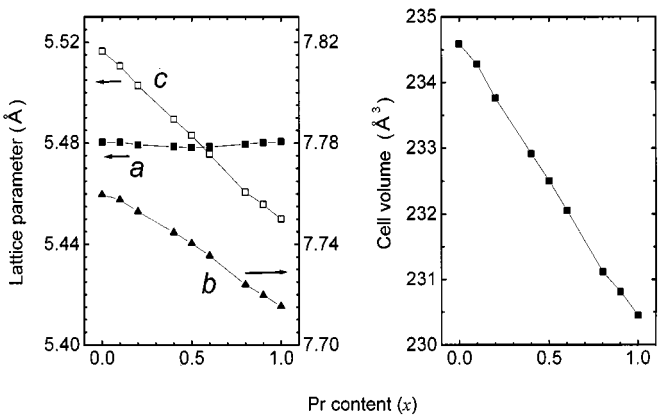

FIG. 1. Lattice parameters and cell volume obtained from the Rietveld analysis for $La_{1-x}Pr_xCrO_3$ ($0 \le x \le 1$) plotted against x. The space group assumed is orthorhombic *Pnma*.

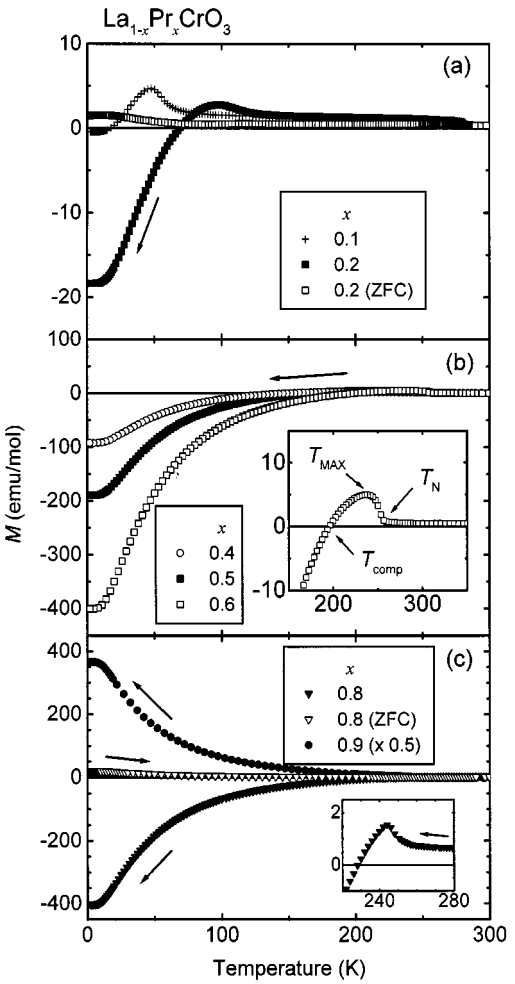

FIG. 2. M–T curves for $La_{1-x}Pr_xCrO_3$ with $0.1 \le x \le 0.9$ in an applied field of $H = 100$ Oe. All the curves were measured in field-cooled (FC) mode except $x = 0.2$ and $x = 0.8$, for which zero-field-cooled (ZFC) curves are also shown. The insets in Figs. 2b and 2c show the FC curves around transition temperatures for $x = 0.6$ and $x = 0.8$, respectively. The definitions for the three transition temperatures of T_N, T_{MAX}, and T_{comp} are noted in the text. Magnetization for $x = 0.9$ (Fig. 2c) was multiplied by a factor of $\frac{1}{2}$.

Figures 2a–2c show the magnetization–temperature (M–T) curves only for the solid solution compounds $La_{1-x}Pr_xCrO_3$ with $0.1 \le x \le 0.9$ measured with an applied field (H) of 100 Oe. Though both field-cooled (FC) and zero-field-cooled (ZFC) curves were measured for each compound, the former curves are mainly shown. The curves for the end compounds $LaCrO_3$ ($x = 0$) and $PrCrO_3$ ($x = 1$) are not shown here, but were shown in a previous paper for both ZFC and FC cases (9). The canted-antiferromagnetic order is observed at $T_N \sim 288$ K and ~ 240 K for $LaCrO_3$ ($x = 0$) and $PrCrO_3$ ($x = 1$), respectively. For these compounds, the FC magnetization exhibited positive values and lies above the ZFC magnetization (9). These are the behaviors of the magnetic materials usually observed. For some

samples of these compounds, ZFC magnetization exhibited negative polarity. This can be understood in terms of random orientation of magnetic domains after zero-field-cooling. The curve profile for $PrCrO_3$ ($x = 1$) resembles that of $La_{0.1}Pr_{0.9}CrO_3$ ($x = 0.9$, Fig. 2c) where the inflection at ~ 70 K might be due to the order of Pr^{3+} moments. Such an anomaly is not apparently observed below T_N for $LaCrO_3$ ($x = 0$) where the La^{3+} ion has no localized $4f$ electron ($4f^0$).

The figures indicate that each solid solution also exhibits a canted-antiferromagnetic transition at T_N between ~ 288 K and ~ 240 K, accompanied by the increase in magnetization. This is noticed for $La_{0.9}Pr_{0.1}CrO_3$ ($x = 0.1$) and $La_{0.8}Pr_{0.2}CrO_3$ ($x = 0.2$) in Fig. 2a, $La_{0.4}Pr_{0.6}CrO_3$ ($x = 0.6$) in Fig. 2b (inset), and $La_{0.2}Pr_{0.8}CrO_3$ ($x = 0.8$) in Fig. 2c (inset). For $La_{0.6}Pr_{0.4}CrO_3$ ($x = 0.4$), the transition profiles are nearly identical to those for $La_{0.4}Pr_{0.6}CrO_3$ ($x = 0.6$) and $La_{0.5}Pr_{0.5}CrO_3$ ($x = 0.5$) (9). The value of T_N monotonically decreases with x, which can be understood in connection with the continuous change of a Cr^{3+}–O^{2-}–Cr^{3+} angle governing the antiferromagnetic interaction between Cr^{3+}. The FC and ZFC curves considerably deviate below T_N because of the irreversibility of magnetic order, as seen for $La_{0.8}Pr_{0.2}CrO_3$ ($x = 0.2$, Fig. 2a) and $La_{0.2}Pr_{0.8}CrO_3$ ($x = 0.8$, Fig. 2c). The regions above T_N obeyed the Curie–Weiss law as for $x = 0.5$ (9). The paramagnetic moments calculated were close (typically $\sim 95\%$) to those estimated from the contribution of a spin-only Cr^{3+} ($\mu_{eff} = 3.87\ \mu_B$) and a free-ion Pr^{3+} ($\mu_{eff} = 3.62\ \mu_B$ (10)) moments. Thus, orbital moments of the Cr^{3+} ions are assumed to be almost quenched in this region.

The curve for $La_{0.9}Pr_{0.1}CrO_3$ ($x = 0.1$) exhibits a broad magnetization peak at 40–50 K as seen in Fig. 2a. This has also been observed for the ZFC curves not shown here. Below ~ 17 K, the polarity of the FC magnetization becomes negative. The negative FC magnetizations are ca. -0.4 emu/mol, whose absolute value is roughly $\sim 1/10$ compared to the peak magnetization at 40–50 K. This phenomenon has not been observed for $LaCrO_3$ ($x = 0$), implying the modification of a magnetic structure caused by the Pr substitution of 10%. In contrast, the curve profile for $La_{0.1}Pr_{0.9}CrO_3$ ($x = 0.9$) shown in Fig. 2c is similar to that of $PrCrO_3$ ($x = 1$) (Fig. 2 in Ref. (9)), indicating that the magnetic order of $PrCrO_3$ remains in the case of the 10% La substitution.

The characteristic point in the present figures is that the solid solutions with $0.2 \leq x \leq 0.8$ exhibit distinct negative magnetization. Some of the features of this phenomenon have been noted in the previous paper on $La_{0.5}Pr_{0.5}CrO_3$ ($x = 0.5$) (9). With cooling of the samples in the FC mode, the magnetization shows a maximum value (M_{MAX}) with a positive polarity at the peak temperatures (T_{MAX}) between ~ 50 K ($x = 0.1$) and ~ 240 K ($x = 0.8$), which are lower than T_N. This situation is recognized only for $x = 0.1$ and 0.2 (Fig. 2a), $x = 0.6$ (inset in Fig. 2b), and $x = 0.8$ (inset in Fig. 2c). The T_{MAX} value tends to shift to higher temperatures with increasing x. Further cooling leads to the compensation temperatures (T_{comp}) where the magnetization becomes zero, as can be seen for $x = 0.2$ (Fig. 2a), $x = 0.6$ (inset in Fig. 2b), and $x = 0.8$ (inset in Fig. 2c). This temperature becomes higher from ~ 17 K ($x = 0.1$) to ~ 230 K ($x = 0.8$) with increasing x up to 0.8. Below T_{comp}, the polarity of the magnetization is negative. The FC magnetization continues to monotonically decrease with cooling until 2 K. Therefore, the FC curves are located far below the ZFC curves as demonstrated for $x = 0.2$ (Fig. 2a) and $x = 0.8$ (Fig. 2c), which is not the normal behavior of magnetic materials. Absolute values of the minimum magnetization (M_{MIN}) are much larger than those of M_{MAX}. The largest value of the absolute magnetization ratio of M_{MIN}/M_{MAX} was obtained for $La_{0.2}Pr_{0.8}CrO_3$ ($x = 0.8$), which is as large as ~ 250. The absolute M_{MIN} value tends to increase with increasing x up to 0.8, plausibly suggesting the contribution of the Pr^{3+} moments. This value for $La_{0.2}Pr_{0.8}CrO_3$ ($x = 0.8$) at 2 K corresponds to $\sim 0.07\ \mu_B$/unit formula.

Another unique point is that distinct negative FC magnetization is observed for the wide composition region of $0.2 \leq x \leq 0.8$, indicating drastic alternation of magnetic structures brought about by the 20% substitution of the lanthanide ions. Though the same qualitative behavior has been reported for a few systems such as $LaVO_3$ (13–15) and $Co[CoV]O_4$ (16), it is characteristic of the present system that the absolute values of M_{MIN} are much larger than those of M_{MAX}. Below T_{comp}, the direction of the magnetization is opposite that of the applied field. Such a state is not in thermal equilibrium. To see the stability of this state, magnetization was measured against time for some compounds with $0.2 \leq x \leq 0.8$ at 4.5 K (much below T_{comp}) in the applied field of 100 Oe, immediately after the FC cooling in the 100-Oe field. The magnetization slightly increased with the lapse of time, approaching a true equilibrium state. The measurements during several hours revealed that the change of magnetization was less than $\sim 1\%$. This stability is an analogous property to that in $GdCrO_3$ (11).

Figure 3 shows magnetization–applied field (M–H) curves for $La_{0.5}Pr_{0.5}CrO_3$ ($x = 0.5$), which were measured at 2 K. The existence of magnetic order for all the compounds was confirmed by observing magnetic hysteresis as shown here. The lack of saturation magnetization is ascribed to the canted-antiferromagnetic order. The curve B measured after field-cooling lies slightly below the curve A measured after zero-field-cooling. Therefore, the memory of the negative magnetization after the field-cooling cannot be completely destroyed, even by the maximum applied field of 50,000 Oe. The same qualitative phenomenon was observed also for $La_{0.6}Pr_{0.4}CrO_3$ ($x = 0.4$) and $La_{0.2}Pr_{0.8}CrO_3$ ($x = 0.8$).

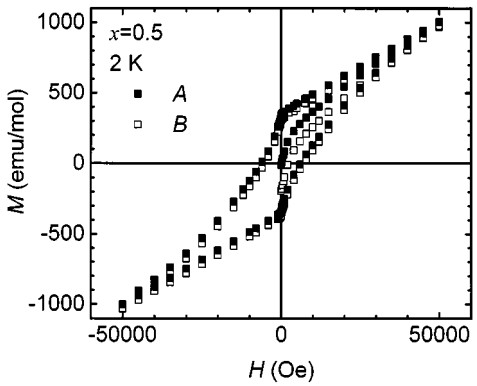

FIG. 3. M–H curves for $La_{0.5}Pr_{0.5}CrO_3$ measured at 2 K. The curve A was measured after zero-field-cooling. The other curve, B, was measured after field-cooling with the applied field of 100 Oe.

As was found for $La_{0.5}Pr_{0.5}CrO_3$ (9), the negative magnetization disappears in high magnetic fields. Figure 4 demonstrates this behavior for one of the other systems. dc susceptibility–temperature (χ–T) curves for $La_{0.8}Pr_{0.2}CrO_3$ ($x = 0.8$) are shown, which were measured with several applied fields (H) in the FC mode. The susceptibility χ is given by M/H (M, magnetization; H, applied field). With increasing applied field H, the absolute values of negative susceptibilities below T_{comp} monotonically decrease, accompanied by the monotonic decrease in T_{comp}. This result plausibly means that the Zeeman energy of the high applied field overcomes the magnetic interactions between the localized moments and magnetic domains, in relation to which no further details can be discussed from the present data alone. In higher fields than the threshold value of ~ 3000 Oe, no negative susceptibility is observed in the whole temperature region. Qualitatively, an identical phenomenon has been observed for $0.2 \leq x \leq 0.8$, where the threshold applied field is different in each system between 3000 and 7000 Oe. This field seemed to show the maximum of 5000–7000 Oe around the Pr contents (x) of $x = 0.4$–0.6.

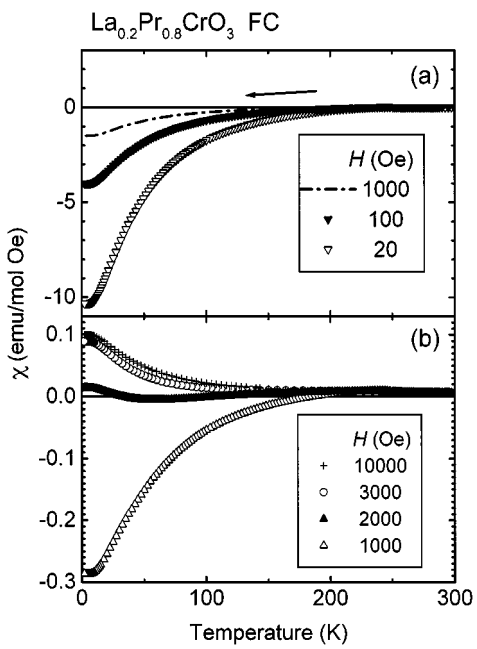

FIG. 4. χ–T curves for $La_{0.2}Pr_{0.8}CrO_3$ with several different applied fields, measured in FC mode. The susceptibility is defined as M/H (M, magnetization; H, applied field).

The profile of each FC curve with $0.2 \leq x \leq 0.8$ below T_{comp} shown in Fig. 2 is similar to that of $GdCrO_3$ ($T_N \sim 170$ K) above 25 K measured in low applied fields of ~ 100 Oe (11), below which the upturn of magnetization leads to another compensation temperature of ~ 17 K. From the magnetization study on a single crystal (8), this negative magnetization was understood in connection with the opposite direction of the Gd^{3+} moment to that of the canted Cr^{3+} moment (11). The similar curve profile implies the same magnetic structure in the present system. To observe the magnetic structures at low temperatures, neutron diffraction measurements were performed for $La_{0.5}Pr_{0.5}CrO_3$. The data taken at 4 K is shown in Fig. 5. The data at room temperature (not shown) could be fitted with the lattice parameters of $a = 5.4736(3)$ Å, $b = 7.7339(3)$ Å, and $c = 5.4818(3)$ Å (space group *Pnma*, goodness-of-fit (S) = 1.37). They are close to those obtained from XRD in Fig. 1. The fitting parameters at 4 K obtained from Fig. 5 are shown in Table 1. The lattice lengths of $a = 5.4722(2)$ Å, $b = 7.7255(3)$ Å and $c = 5.4740(2)$ Å are shorter than those at room temperature. The unit-cell shrinkage caused by the sample cooling was confirmed from the measurements at 170 and 220 K where the fit was done assuming also *Pnma*. The same space group below T_N implies that a crystallographic change, like that proposed for $LaVO_3$ (15), is not responsible for the negative magnetization effect.

In the figure, magnetic peaks are most distinctly observed around $2\theta = 23.5°$, where the contribution of nuclear Bragg reflections is almost zero. In the refinement, both G_y- and G_z-type antiferromagnetic spin configurations (17) of Cr^{3+} were attempted like for the end compound $PrCrO_3$ (5, 18). These two configurations have been reported for the magnetic structure of Cr^{3+} in $PrCrO_3$ (5,18), mainly because of the complexity that the two magnetic peaks are located almost at the same angle (18). This situation was found also in the present data; i.e., the two reflections of (011) and (110) appear at almost the same angle of $2\theta \sim 23.5°$. A slightly smaller goodness-of-fit (S) indicator was obtained for G_y than for G_z. The magnetic structure proposed here is shown in Fig. 6. Magnetization measurements on a single-crystal $PrCrO_3$ support the configuration of G_y (G_z for *Pbnm*) (19). The ordered Cr^{3+} moment obtained, 2.50(5) μ_B, is close to that of 2.45–2.46 μ_B for $PrCrO_3$ at 4.2 K (5, 18). It is relevant that this moment decreases with the increase in

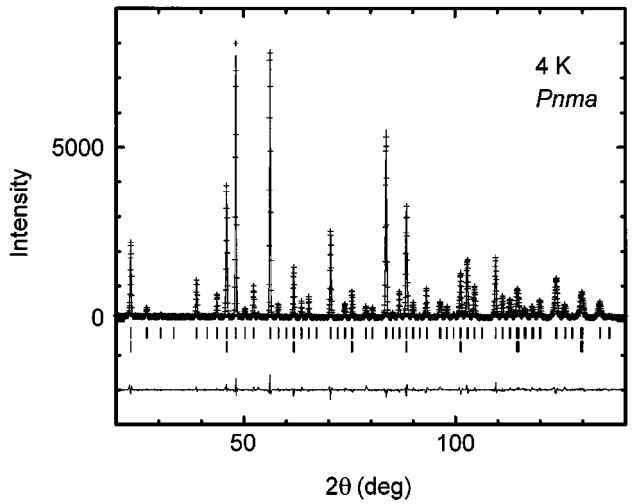

FIG. 5. Powder neutron diffraction patterns for $La_{0.5}Pr_{0.5}CrO_3$ (space group *Pnma*) at 4 K. The experimental and calculated data are shown as the cross markers and the upper solid line, respectively. The upper and lower vertical markers stand for nuclear and magnetic Bragg reflections, respectively. The lower solid line shows the difference between the experimental and calculated data. Fitting parameters are shown in Table 1.

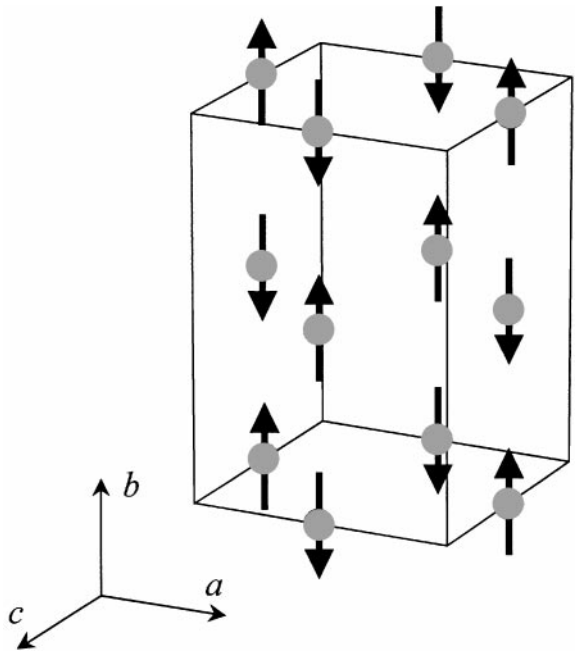

FIG. 6. Magnetic structure for $La_{0.5}Pr_{0.5}CrO_3$ at 4 K proposed from powder neutron diffraction. The Cr^{3+} ions are shown as the spheres. The other ions are omitted. Ordered Cr^{3+} moments of 2.50(5) μ_B along the *b* axis are shown as the arrows.

temperature, i.e., 2.11(2) μ_B at 170 K and 1.70(2) μ_B at 220 K. Neither the canted Cr^{3+} order nor the Pr^{3+} order could be detected with accuracy, both of which are expected to have an *F*-type (17) (ferromagnetic) configuration considering the existence of the canted Cr moment. This result is explained in connection with the small magnetization around 4 K, which is deduced from Fig. 2. The absolute magnetization around 4 K corresponds to ~ 0.04 μ_B/unit formula in the case of 100 Oe. A similar value of ~ 0.06 μ_B/unit formula is obtained from the remanent magnetization shown in Fig. 3. Judging from the fact that the Dzyaloshinsky vector is parallel to the *a* axis in *Pnma* (20), the G_y configuration provides the parallel component of the canted Cr^{3+} moment to the *c* axis (i.e., F_z mode).

It was proposed for $GdCrO_3$ that the measured moment $\boldsymbol{M}$ in the FC process could be expressed in the following formula (8, 11):

$$\boldsymbol{M} = \boldsymbol{M}_{\mathbf{Cr}} + C(\boldsymbol{H}_I + \boldsymbol{H})/(T - \theta). \quad (1)$$

Here, $\boldsymbol{M}_{\mathbf{Cr}}$, C, $\boldsymbol{H}_I$, $\boldsymbol{H}$, and θ stand for the canted moment of Cr^{3+}, a Curie constant, an internal field from Cr^{3+}, an applied field, and a Weiss temperature, respectively. The Curie constant C was fixed to be that calculated from the free Gd^{3+} moment. The values of $\boldsymbol{M}_{\mathbf{Cr}}$, $\boldsymbol{H}_I$, and θ obtained for $GdCrO_3$ were ~ 100 emu/mol, ca. -1900 Oe, and ca. -13 K, respectively (11). Figure 7 demonstrates that this formula could be applied also to the present data. The effective paramagnetic moment of Pr^{3+} adopted here was 3.62 μ_B (10), involving the effect from thermally excited states. The deviation below ~ 30 K where no suitable fit has been attained is considered to originate from the combined effect of both a crystal field around Pr^{3+} (21) and a tendency toward magnetic order of Pr^{3+} as seen in $PrCrO_3$ (5, 18). The values of $\boldsymbol{M}_{\mathbf{Cr}}$, $\boldsymbol{H}_{\mathbf{I}}$, and θ obtained here are ~ 40 emu/mol, ca. -8500 Oe, and ca. -3 K, respectively. The very small $\boldsymbol{M}_{\mathbf{Cr}}$ corresponding to ~ 0.007 μ_B/Cr^{3+} is in qualitative agreement with the small canting angle of Cr^{3+} in the end compound $PrCrO_3$, 18 mrad (19). Different parameter values obtained for the applied fields of 20 and 1000 Oe indicate their field dependence in a low-field region, i.e., $\boldsymbol{M}_{\mathbf{Cr}}$, $\boldsymbol{H}_{\mathbf{I}}$, and θ were ~ 20–70 emu/mol, ca. -4000–13000 Oe, and ca. -7 K, respectively. This fit could not be performed well for the higher fields, which

TABLE 1
Crystal and Magnetic Structures for $La_{0.5}Pr_{0.5}CrO_3$ at 4 K Obtained from Powder Neutron Diffraction

Atom	Position	*x*	*y*	*z*	*B* (Å^2)
La/Pr	4*c*	0.0285(3)	0.25	−0.0043(6)	0.19(4)
Cr	4*b*	0.0	0.0	0.5	0.07(5)
O(1)	4*c*	0.4859(5)	0.25	0.0675(6)	0.42(7)
O(2)	8*d*	0.2159(4)	0.5395(2)	0.2208(3)	0.12(4)

Note. $La_{0.5}Pr_{0.5}CrO_3$ at 4 K (space group *Pnma*); $a = 5.4722(2)$, $b = 7.7255(3)$, and $c = 5.4740(2)$ Å; ordered moment of Cr^{3+}: 2.50(5) μ_B along the *b* axis (G_y type); $R_{WP} = 8.68$, $R_I = 2.57$, $R_F = 1.64\%$, goodness-of-fit (S) = 1.40.

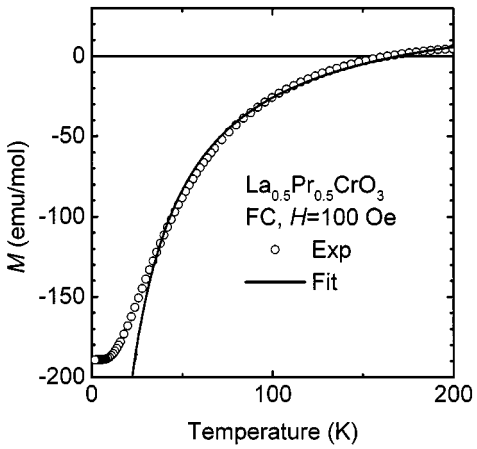

FIG. 7. M–T curves for $La_{0.5}Pr_{0.5}CrO_3$ with $H = 100$ Oe. Experimental data taken in FC mode is labeled as Exp. The solid line (Fit) means a Curie–Weiss-type fit for the Pr^{3+} moment, whose details are in the text.

might be because of the change of magnetic structures depending on both temperature and applied field. Comparably similar parameters were obtained also for the compounds with $x = 0.4$, 0.6, and 0.8. Only the absolute $\boldsymbol{H}_{\mathbf{I}}$ value exhibited composition dependence; i.e., it tended to slightly increase with increasing x. This is consistent with the increase in the absolute value of the negative magnetization with increasing x up to 0.8 as seen in Fig. 2. For the other solid solutions with $x = 0.1$ and 0.2 exhibiting negative magnetization, the formula could not be applied due to complex temperature dependence of the magnetization. From these results, our present speculation is that the negative magnetization is brought about by the paramagnetic effect of the Pr^{3+} moments, at least, in the composition region of $\sim 0.4 < x < \sim 0.8$. Since the values of $\boldsymbol{M}_{\mathbf{Cr}}$ and $\boldsymbol{H}_{\mathbf{I}}$ were estimated from the spatially averaged magnetization in the polycrystalline samples, magnetization measurements on single crystals would be necessary, which might elucidate also the details of complex temperature and field dependence of magnetization. It is worth noting that the antiparallel coupling between Pr^{3+} and the canted Cr^{3+} moments was suggested also for the end compound $PrCrO_3$ (19), where no negative FC magnetization was observed. The increase in T_{comp} with increasing x up to 0.8 noted earlier is qualitatively interpreted in terms of the increase in the Curie constant C (Eq. [1]) caused by the increase in both the Pr content and the absolute $\boldsymbol{H}_{\mathbf{I}}$ value.

The negative FC magnetization only in the solid solutions may have a correlation with the weakening of anisotropy around Pr^{3+}, arising from the substitution of nonmagnetic La^{3+} ($4f^0$). Namely, the Pr^{3+} moments can rotate easily in the direction of the internal field from Cr^{3+} because of a weaker anisotropic effect than that in the end compound $PrCrO_3$. This explanation might be applicable for $GdCrO_3$ where Gd^{3+} has no degree of freedom of an orbital quantum number ($L = 0$) in the ground state ($4f^7$). However, to reveal the true origin of the characteristic behavior of the present system, further studies are apparently needed in the future.

ACKNOWLEDGMENTS

We gratefully thank Dr. Y. Shimojo of JAERI for the neutron diffraction measurements. Dr. T. Inami of JAERI is also greatly acknowledged for his help in the analysis of the neutron diffraction data.

REFERENCES

1. J. B. Goodenough and J. M. Longo, *in* "Magnetic and Other Properties of Oxides and Related Compounds," Landolt-Bornstein, Group III, Vol. 4, p. 126. Springer-Verlag, New York, 1970.
2. S. Nomura, in "Magnetic and Other Properties of Oxides and Related Compounds," Landolt-Bornstein, Group III, Vol. 12, p. 368. Springer-Verlag, New York, 1978.
3. C. P. Khattak and D. E. Cox, *Mater. Res. Bull.* **12,** 463 (1977).
4. T. Arakawa, S. Tsuchi-ya, and J. Shiokawa, *Mater. Res. Bull.* **16,** 97 (1981).
5. E. F. Bertaut, J. Mareschal, G. de Vries, R. Aleonard, R. Pauthenet, J. P. Rebouillat, and V. Zarubicka, *IEEE Trans. Mag.* **2,** 453 (1966).
6. H. Taguchi, M. Nagao, and Y. Takeda, *J. Solid State Chem.* **114,** 236 (1995), doi:10.1006/jssc.1995.1034.
7. K. Tezuka, Y. Hinatsu, A. Nakamura, T. Inami, Y. Shimojo, and Y. Morii, *J. Solid State Chem.* **141,** 404 (1998), doi:10.1006/jssc.1998.7961.
8. A. H. Cooke, D. M. Martin, and M. R. Wells, *J. Phys. C*: *Solid State Phys.* **7,** 3133 (1974).
9. K. Yoshii and A. Nakamura, *J. Solid State Chem.* **155,** 447 (2000), doi:10.1006/jssc.2000.8943.
10. J. H. Van Vleck, "The Theory of Electric and Magnetic Susceptibilities," Oxford Univ. Press, London, 1965.
11. K. Yoshii, *J. Solid State Chem.* **159,** 204 (2001), doi:10.1006/jssc.2000.9152.
12. F. Izumi and T. Ikeda, *Mater. Sci. Forum* **321–324,** 198 (2000).
13. A. V. Mahajan, D. C. Johnston, D. R. Torgeson, and F. Borsa, *Phys. Rev. B* **46,** 10966 (1992).
14. N. H. Hur, S. H. Kim, K. S. Yu, Y. K. Park, J. C. Park, and S. J. Kim, *Solid State Commun.* **92,** 541 (1994).
15. H. C. Nguyen and J. B. Goodenough, *Phys. Rev. B* **52,** 324 (1995).
16. N. Menyuk, K. Dwight, and D. G. Wickham, *Phys. Rev. Lett.* **4,** 119 (1960).
17. E. F. Bertaut, *Acta. Crystallogr. A* **24,** 217 (1968).
18. N. Shamir, H. Shaked, and S. Shtrikman, *Phys. Rev. B* **24,** 6642 (1981).
19. J. D. Gordon, R. M. Hornreich, S. Shtrikman, and B. M. Wanklyn, *Phys. Rev. B* **13,** 3012 (1976).
20. G. Amow, J.-S. Zhou, and J. B. Goodenough, *J. Solid State Chem.* **154,** 619 (2000), doi:10.1006/jssc.2000.8905.
21. E. D. Jones, *Phys. Rev.* **180,** 455 (1969).